

This discussion paper is/has been under review for the journal Atmospheric Chemistry and Physics (ACP). Please refer to the corresponding final paper in ACP if available.

Discrimination of water, ice and aerosols by light polarisation in the CLOUD experiment

L. Nichman¹, C. Fuchs², E. Järvinen³, K. Ignatius⁴, N. F. Höppel³, A. Dias⁵, M. Heinritzi⁶, M. Simon⁶, J. Tröstl², A. C. Wagner⁶, R. Wagner⁷, C. Williamson^{6,a,c}, C. Yan⁷, F. Bianchi^{2,8}, P. J. Connolly¹, J. R. Dorsey¹, J. Duplissy⁹, S. Ehrhart⁵, C. Frege², H. Gordon⁵, C. R. Hoyle^{2,10}, T. B. Kristensen⁴, G. Steiner^{7,11,b}, N. M. Donahue¹², R. Flagan¹³, M. W. Gallagher¹, J. Kirkby^{5,6}, O. Möhler³, H. Saathoff³, M. Schnaiter³, F. Stratmann⁴, and A. Tomé¹⁴

¹School of Earth, Atmospheric and Environmental Sciences, University of Manchester, Manchester, M13 9PL, UK

²Laboratory of Atmospheric Chemistry, Paul Scherrer Institut, 5232 Villigen, Switzerland

³Karlsruhe Institute of Technology, Institute for Meteorology and Climate Research, P.O. Box 3640, 76021 Karlsruhe, Germany

⁴Institute for Tropospheric Research (TROPOS), 04318 Leipzig, Germany

⁵CERN, PH Department, Geneva, Switzerland

⁶Institute for Atmospheric and Environmental Sciences, Goethe-University Frankfurt, Frankfurt am Main, Germany

Discrimination of
water, ice and
aerosols by light
polarisation

L. Nichman et al.

Title Page

Abstract

Introduction

Conclusions

References

Tables

Figures

⏪

⏩

◀

▶

Back

Close

Full Screen / Esc

Printer-friendly Version

Interactive Discussion



⁷Department of Physics, University of Helsinki, P.O. Box 64, 00014 University of Helsinki, Finland

⁸Switzerland Institute for Atmospheric and Climate Science, ETH Zurich, 8092 Zurich, Switzerland

⁹Helsinki Institute of Physics, Finland

¹⁰Swiss Federal Institute for Forest Snow and Landscape Research (WSL)-Institute for Snow and Avalanche Research (SLF), Davos, Switzerland

¹¹Ion Molecule Reactions & Environmental Physics Institute of Ion Physics and Applied Physics Leopold-Franzens University, Innsbruck, Austria

¹²Center for Atmospheric Particle Studies, Carnegie Mellon University, Pittsburgh PA 15213 USA

¹³California Institute of Technology, Division of Chemistry and Chemical Engineering, Pasadena, California 91125, USA

¹⁴CENTRA-SIM, University of Lisbon and University of Beira Interior, 1749-016 Lisbon, Portugal

^anow at: Chemical Sciences Division NOAA Earth System Research Laboratory, Boulder, Colorado, USA

^bnow at: Aerosol Physics and Environmental Physics Faculty of Physics, University of Vienna, Wien, Austria

^calso at: Cooperative Institute for Research in Environmental Sciences, University of Colorado Boulder, Boulder, Colorado, USA

Received: 18 September 2015 – Accepted: 28 October 2015 – Published: 10 November 2015

Correspondence to: L. Nichman (leonid.nichman@manchester.ac.uk)

Published by Copernicus Publications on behalf of the European Geosciences Union.

Discrimination of water, ice and aerosols by light polarisation

L. Nichman et al.

Title Page

Abstract

Introduction

Conclusions

References

Tables

Figures



Back

Close

Full Screen / Esc

Printer-friendly Version

Interactive Discussion



Abstract

Cloud microphysical processes involving the ice phase in tropospheric clouds are among the major uncertainties in cloud formation, weather and General Circulation Models (GCMs). The simultaneous detection of aerosol particles, liquid droplets, and ice crystals, especially in the small cloud-particle size range below 50 μm , remains challenging in mixed phase, often unstable ice-water phase environments. The Cloud Aerosol Spectrometer with Polarisation (CASPOL) is an airborne instrument that has the ability to detect such small cloud particles and measure their effects on the backscatter polarisation state. Here we operate the versatile Cosmics-Leaving-Outdoor-Droplets (CLOUD) chamber facility at the European Organisation for Nuclear Research (CERN) to produce controlled mixed phase and other clouds by adiabatic expansions in an ultraclean environment, and use the CASPOL to discriminate between different aerosols, water and ice particles. In this paper, optical property measurements of mixed phase clouds and viscous Secondary Organic Aerosol (SOA) are presented. We report observations of significant liquid – viscous SOA particle polarisation transitions under dry conditions using CASPOL. Cluster analysis techniques were subsequently used to classify different types of particles according to their polarisation ratios during phase transition. A classification map is presented for water droplets, organic aerosol (e.g., SOA and oxalic acid), crystalline substances such as ammonium sulphate, and volcanic ash. Finally, we discuss the benefits and limitations of this classification approach for atmospherically relevant concentration and mixtures with respect to the CLOUD 8–9 campaigns and its potential contribution to Tropical Troposphere Layer (TTL) analysis.

Discrimination of water, ice and aerosols by light polarisation

L. Nichman et al.

Title Page

Abstract

Introduction

Conclusions

References

Tables

Figures



Back

Close

Full Screen / Esc

Printer-friendly Version

Interactive Discussion



1 Introduction

Scattering and absorption due to atmospheric particles can vary widely, leading to net radiative effect that either cool or warm the surface of the Earth. Ice crystals pose a potential challenge since their non-sphericity complicates the theoretical description of their single scattering properties (Macke et al., 1996). Several attempts have been made to model and simulate light interactions with different ice crystal habits, mixtures of crystal types, aggregates, and aerosols (Baran, 2013), but no single method can easily combine all size ranges and types of particles, making accurate, unified modelling nearly impossible.

Scattering analysis is complicated further in small ice crystals and Secondary Organic Aerosol (SOA). Small ice crystals can have different major internal defects (e.g., stacking faults, chemical defects, molecular vacancies, interstitial molecules, ionized states, and orientation defects), surface roughness, and branching with various symmetries; the optical effects of these defects depend strongly on the spatial orientation of the particle in a flow. They can lead to systematic biases since particles with a high width to height aspect ratio can have a preferred orientation in chamber measurements. However, single particle-by-particle analysis of the backscatter polarisation state is useful for particle discrimination as we shall show.

Aerosol particles found in the lower confines of the atmosphere are typically internal or external mixtures of inorganic salts, refractory components such as mineral dusts and clays, and organic species; they also contain varying quantities of water. Organic components create hygroscopicity variation that affect the water uptake of the particles (Cziczo et al., 2004; Jimenez et al., 2009; Duplissy et al., 2011). Water uptake variation between pure sulphate and internally mixed organic/sulphate aerosols alter the particle refractive index and may lead to mis-sizing by optical instruments if the composition is not taken into account (see Sect. 2.3). In addition to the familiar liquid and crystalline states, atmospheric aerosol may also exist in semi-solid and solid amorphous states (i.e., lacking an ordered, repeating structure) such as soft polymers, gels, or glasses

Discrimination of water, ice and aerosols by light polarisation

L. Nichman et al.

Title Page

Abstract

Introduction

Conclusions

References

Tables

Figures



Back

Close

Full Screen / Esc

Printer-friendly Version

Interactive Discussion



Discrimination of water, ice and aerosols by light polarisation

L. Nichman et al.

Title Page

Abstract

Introduction

Conclusions

References

Tables

Figures



Back

Close

Full Screen / Esc

Printer-friendly Version

Interactive Discussion



314 cm once across the middle plane of the CLOUD chamber. Thus, this instrument provides the RH also in the presence of clouds. Subtracting the water vapour content from the total water content results in the condensed (ice or liquid) water content. Sulphuric acid, ammonium sulphate, and oxalic acid particles were used to seed the chamber with CCN concentrations ranging from 0.5 to several thousand particles cm^{-3} . The CCN number concentrations determined the cloud droplet size, with higher CCN concentration producing higher concentrations of smaller ice particles in CLOUD.

Although the expansion is, ideally, adiabatic, heat is continuously transferred to the cooled air from the chamber walls, as the temperature control system is maintained at the pre-expansion temperature, resulting in eventual evaporation of the cloud. The cloud lifetime in the CLOUD experiments could be controlled (e.g., by fan speed or by number of steps in the expansion profile) from several minutes to greater than forty minutes when required (e.g., for ice evolution experiments).

2.2 Cloud Experiment overview

A series of experiments was conducted to generate liquid clouds (Hoyle et al., 2015), mixed phase clouds, and pure ice clouds. Controlling stepwise the rate of expansion and the humidity flow into the chamber in the mixed phase experiments, it was possible to obtain water super saturation followed by ice super saturation, allowing CCN activation to form a cloud for a short period of several minutes. The adiabatic expansion experiments on which this paper focuses are summarised in Table 1, but results based on a much broader data base of several hundred CLOUD expansions will also be considered for the discussions.

Several additional experiments were conducted to examine any aerosol polarisation state changes arising from possible viscosity changes in response to RH variations, using CASPOL. A more detailed description of the latter can be found in the accompanying paper by Järvinen et al. (2015).

2.3 The CAPS-CASPOL instrument

The Cloud and Aerosol Spectrometer with Polarisation detection (CASPOL) is part of the Cloud Aerosol and Precipitation Spectrometer (CAPS). The first variant of the instrument was introduced in 1999 and was designed for airborne in situ cloud measurements (Baumgardner et al., 2001; Heymsfield, 2007), although it has subsequently been used for cloud chamber measurements (Krämer 2009). The version of CASPOL employed here has a linearly polarised laser to provide a collimated incident beam of light at a wavelength of 680 nm. There are four detectors in the instrument, with collection angles of 4 to 12° for the forward detectors and 168 to 176° for the backward detectors. The near forward angles are used because most of the light scattered from a particle whose diameter is larger than the incident wavelength is in the forward direction. The backscattering signal is used for qualitative particle shape discrimination. The CASPOL has an additional back-scatter detector with a polarised filter (90° to the polarisation of the incident light) to measure the change in polarisation of scattered light caused by aspherical particles (Baumgardner et al., 2011; Glen and Brooks, 2013). In this configuration, spherical particles produce little response in the perpendicular polarisation backscatter detector. Conversely, frozen water droplets and aspherical ice crystals will show much more distinct signals. The particle's water equivalent optical diameter is determined from the forward scattering signal using the standard Mie scattering assumptions, i.e., spherical geometry and isotropic refractive index. An additional detector in the forward direction is used as a qualifier; it has a rectangular optical mask that restricts scattered light from particles that are outside the centre of focus of the laser beam. Only particles within the optimal view volume are counted and characterized. All data are collected on a single particle basis, thus provide a measure of particle-by-particle variability and single particle optical properties. In order to eliminate aerosol particle interference in our cloud measurements, only contributions from a subset of larger particles above 3 µm were included. This threshold is based on work by Baumgardner et al. (2001) and Lance (2012) who selected a similar size range for

cloud particle measurements. In the special case of SOA measurements, a subset of small particles ($< 3 \mu\text{m}$) detected in the lower gain stage, was considered.

Calibration

Size calibration of CASPOL, as described in Rosenberg et al. (2012), relates the amplitude of the instrument's response to particle scattering cross-sections. Using the Mie-Lorenz curve, the nominal size bin limits can then be defined in terms of the diameter of water droplets having the same scattering cross-section, giving a reasonable estimate of particle size for liquid droplets and small spherical ice particles. Aspherical particles will be mis-sized with respect to spherical particle, subject to their cross-section as shown by Borrmann et al. (2000). In our instrument the error would normally be in the order of the size bin width.

2.4 Data processing

2.4.1 Particle-by-particle analysis

The polarisation ratio measured with the CASPOL instrument and reported in this paper is defined as the ratio of perpendicularly polarised backscatter intensity to total backscatter intensity and provides a measure of phase, composition, and surface features of the particle. This ratio differs from the depolarisation ratio that is measured using remote sensing techniques (Groß et al., 2013). The two ratios cannot be directly compared, requiring additional calibration for this purpose (Meyer, 2011). The ratio of perpendicularly polarised backscatter to forward scatter ($D_{\text{pol}}/F_{\text{wd}}$) indicates the contribution of particle size to the scattering. PBP measurements reveal the fraction of aspherical particles population (Fig. 2c) and its evolution. Here we employ cluster analysis on PBP data (Sect. 2.4.2) for phase discrimination and for data quality assurance. This method can also be used to classify highly polarising particles. Corrections

Discrimination of water, ice and aerosols by light polarisation

L. Nichman et al.

Title Page

Abstract

Introduction

Conclusions

References

Tables

Figures



Back

Close

Full Screen / Esc

Printer-friendly Version

Interactive Discussion



to the forward, backward and the Dpol channels have been applied and summarized in Table S2 in the Supplement.

2.4.2 Cluster analysis

Clustering or grouping of data by the similarity in one variable or a matrix of variables reveals the size of the population with similar properties and the number of the unique groups in the dataset, as well as the spread in each group. Clustering analysis is used here to discriminate and assign unique particle properties corresponding to different phases during the experiment (e.g., water, ice), primarily based on polarisation differences (Fig. 3). Clustering approaches have been previously used for aerosol property classification, e.g., Omar et al. (2005), Robinson et al. (2013), Crawford et al. (2015). Here we use the MatLab K means cluster function. First the number of clusters, k , is specified. The algorithm then calculates the minimum total intra-cluster variance (Eq. 1)

$$\sum_{i=1}^K \sum_{x_j \in S_i} d(x_j, \mu_i) \quad (1)$$

where S_i is the i th cluster ($i = 1, \dots, K$), μ_i is the i th centroid of all the points x_j in cluster S_i , and d is the distance function (e.g., squared Euclidean). In this case the function is applied to a matrix of parameter vectors including polarisation, size, asphericity, concentration, inter-arrival-time, time, etc. This approach should, by itself, be sufficient for discriminating a simple mixture consisting of two discrete and well-separated phases as may be found in the water-ice particle population. In our aerosol-cloud nucleation experiments, an a-priori assumption of cluster number is challenging due to the variability of particles. Initial estimates of cluster numbers (1–7) were tested in sequential iterations. A silhouette index, $s(i)$, was then used to quantitatively assess the quality of clustering. This is a composite index reflecting the compactness and separation of clusters; a larger average silhouette index indicates a better overall quality of the clustering result (Chen et al., 2002). The silhouette value of a point is a measure of the similarity

Discrimination of water, ice and aerosols by light polarisation

L. Nichman et al.

Title Page

Abstract

Introduction

Conclusions

References

Tables

Figures



Back

Close

Full Screen / Esc

Printer-friendly Version

Interactive Discussion



of points within a given cluster compared to these in other clusters; it is defined as

$$s(i) = \frac{b(i) - a(i)}{\max(a(i), b(i))} \quad (2)$$

where $a(i)$ is the average distance of the point i to the other points in its own cluster A . $d(i, C)$ is the average distance of the point i to the other points in the cluster C . $b(i)$ is the minimal $d(i, C)$ over all clusters other than A (Eq. 2). For the best possible fit, the silhouette index is, $s(i) = 1$. This validation is sufficient for our analysis to indicate the ability of the algorithm to group similar data sets using the prescribed values. Following cluster analysis, asphericity thresholds are selected based on cluster boundaries identified by the colour transition in Fig. 3.

3 Results

3.1 CASPOL water–ice measurements

As the temperature in the chamber decreases in the multistep expansions, liquid cloud starts to form when the RH exceeds water saturation (Fig. 1). Figure 2a shows the formation of a mixed phase cloud as a function of time. Droplets formed at sub-zero temperatures are super-cooled and some of them freeze. During the stabilisation period, when pressure remains constant, some of the super-cooled droplets evaporate as the walls reheat the chamber. During the second step of the expansion, the ice grows further. The rapid growth of ice particles depletes the available water vapour, causing the remaining liquid droplets to evaporate by the Bergeron–Findeisen mechanism. The aspherical fraction (Fig. 2b), and the concentrations of water and ice (Fig. 2c) were calculated from the PBP cluster analysis for each of these conditions during the run. Images of some typical ice particles (diameter < 150 μm) from the Cloudy experiments were captured by the 3VCPI. These diverse experiments produced ice habits that included needles, hexagonal plates, columns, bullets and dendrites; ice aggregates and

spheroids were also detected (Fig. 4). These habits scatter the light differently. However, CASPOL data were in good agreement with ice measurements by the PPD, small water droplets measured with WELAS (Figs. S3 and S4 in the Supplement).

3.2 ACPIM modelling

A modelling tool used in this analysis is the Aerosol–Cloud–Precipitation Interaction Model (ACPIM), which has been developed at the University of Manchester in collaboration with the Karlsruhe Institute of Technology (Connolly et al., 2009). Temperature time series were plotted using the initial experimental conditions (e.g., chamber temperature, pressure, RH, and CCN concentration) in the model. Subsequent fitting of the simulated temperature drop to chamber data enabled us to find the rate at which the chamber reheats after expansion (0.007 s^{-1}) for the runs specified in Table 1. This heat exchange coefficient is in a good agreement with the results found by Dias et al. (2015). It quantifies how effectively heat is transferred from the chamber walls and mixed throughout the gas in this chamber.

ACPIM was able to replicate the observed particle phase transitions in the mixed phase runs, thereby validating the phase concentration plot (Fig. 2c). Phase concentration deviations at the beginning of the expansion were probably caused by inhomogeneity in the chamber due to incomplete mixing, or by variations in the expansion rate. Ambiguous polarisation states of water, e.g., in super-cooled or frozen droplets, might be resolved by comparing ACPIM to CASPOL data and examining the mismatch. This simulation of the experiment makes it possible to predict phase concentrations and sizes, supporting the planning of future experiments and validation of the theories behind the model.

3.3 Viscous SOA measurements

The viscous SOA growth experiments reported here were achieved using a controlled, constant flow of precursor gases and ozone into the chamber at constant, near-ambient

Discrimination of water, ice and aerosols by light polarisation

L. Nichman et al.

Title Page

Abstract

Introduction

Conclusions

References

Tables

Figures



Back

Close

Full Screen / Esc

Printer-friendly Version

Interactive Discussion



Discrimination of water, ice and aerosols by light polarisation

L. Nichman et al.

Title Page

Abstract

Introduction

Conclusions

References

Tables

Figures



Back

Close

Full Screen / Esc

Printer-friendly Version

Interactive Discussion



pressure, dry conditions, and constant temperatures, as shown in Table 2 (for details see Järvinen et al., 2015). We observe a growth in particle diameter from tens of nanometres to more than 1 μm size particles. During these growth periods (Fig. 5), an increase in the CASPOL backscatter polarisation ratio was observed, while the Dpol/Fwd ratio did not change significantly, suggesting the change in size had less effect on the measurements than did the polarisation. A large part of the experiment produced extreme particle concentrations above the recommended CASPOL concentration limit of 1300 cm^{-3} , where significant coincidence errors would be likely to occur (D. Baumgardner, personal communication, 2015). Therefore, we limit our discussion to conditions in which growth to sizes larger than $0.56\text{ }\mu\text{m}$ in diameter, and concentrations below 1300 cm^{-3} occur (for details see Sect. 4). After the growth, RH was increased up to 80 % in each experiment in order to observe the phase transitions using optical depolarisation measurements made with the SIMONE instrument (Järvinen et al., 2015). Several repetitions of these growth experiments followed by humidification and phase transition were conducted. The subsequent glass transition formed liquid particles at the end of each experiment. As concentrations decreased below the CASPOL operating threshold of 1300 cm^{-3} , a significantly lower particle polarisation (more optically spherical) state was detected by the CASPOL. As a consequence, we observed the presence of two distinct polarisation clusters during the growth where highly viscous SOA is expected and after the phase transition where we expect to see liquid particles. The two clusters are overlaid for several experiments as shown in Fig. 6.

While cooling the chamber and reducing the RH (Run #1515.16) (Fig. 7), the larger optically semi-spherical particles started to dry. Oxidized α -pinene SOA compounds generally have added functional groups (oxygen containing substituents), high polarity, and, thus, lower vapour pressure (Pandis et al., 1992) than water. As a result of this drying process and the dynamics of partitioning, CASPOL measures an increase in polarisation. The detailed dynamics of partitioning in SOA from alpha-pinene ozonolysis is described in Donahue et al. (2014).

Discrimination of water, ice and aerosols by light polarisation

L. Nichman et al.

Title Page

Abstract

Introduction

Conclusions

References

Tables

Figures



Back

Close

Full Screen / Esc

Printer-friendly Version

Interactive Discussion



This could be explained as transition to an amorphous aerosol phase with high viscosity at $RH \sim 10\%$, $T = -30$ to -38°C , $P = 102$ kPa as suggested by the hysteresis plot of Koop et al. (2011). Our results cannot, however, be unambiguously ascribed to this based solely on the measurements here. We simply note the ability of the CASPOL to identify very significant polarisation shifts in the aerosol scattering properties that are likely associated with changes in their physico-chemical properties.

Additional support for this hypothesis comes from SMPS measurements. No particles were detected in the SMPS size range in this period; the upper cut-off of the measurement was about 400 nm. Small decay of the averaged diameter is observed in CASPOL (Fig. 8). These data indicate a wet to dry transformation of essentially large particles. This reversed transition of the viscosity is then followed by much slower partitioning or dissociation within these particles, and a decrease in their concentration and sizes due to constantly decreasing RH.

3.4 Particle classification maps

It is clear that classification of particles has wide reaching effects on our understanding of the atmosphere. In order to map the whole range of atmospheric processes under future emissions scenarios, it will be necessary to identify the particles. A new strategy to categorize dust groupings was developed by Glen and Brooks (2013, 2014) whereby optical scattering signatures from CASPOL measurements were used to develop a set of threshold rules based on polarisation ratios. These rules can be used to classify types of dust sampled in the laboratory and during field campaigns. A plot of the total backscatter intensity as a function of the polarisation ratio for various types of dust clearly shows the difference in their signatures. Similar techniques for classifying aerosols are already in use by the Light Detection And Ranging (LIDAR) community (Burton et al., 2012; Petzold et al., 2010). To explore the feasibility of using the signature method in CLOUD, we have collated polarisation ratio ranges of many particles measured in the CLOUD 8 and 9 campaigns. Here we present the polarisation map (Fig. 9) combining the CLOUD campaign measurements with those obtained from air-

Discrimination of water, ice and aerosols by light polarisation

L. Nichman et al.

Title Page

Abstract

Introduction

Conclusions

References

Tables

Figures



Back

Close

Full Screen / Esc

Printer-friendly Version

Interactive Discussion



craft flights over the North sea (Johnson et al., 2012) using the same CASPOL instrument. This map makes it possible to predict the coordinates of other potential organic compounds in the upper area. Salts, ash, and ice are in the mid-range of the Dpol/Bck ratio; spherical liquids are at the bottom. Further separation by size might be possible on the x axis. In comparison between SIMONE and CASPOL for SOA data points from CLOUD, we can see on the map that SOA – CLOUD 8 (+10 °C) data points have lower polarisation ratio compared to other organic aerosols. This measurement implies lower viscosity and could explain the non-existent phase transition in SIMONE depolarisation measurements for this experiment. More experimental data is needed to fill the space for other particles, temperatures and RH.

The classification of ice and water is limited by size. As explained earlier CASPOL can only differentiate between the asphericities of the particles. The ice presented on this map is aspherical. Slight changes in the polarisation state of droplets can be observed as the droplets cool and a crystalline pattern emerges. This discrimination technique could be used in chamber measurements with mixtures of CCN and Ice Nuclei (IN) and with some limitations could be applied in explicit atmospheric measurements albeit with higher uncertainty due to potentially significant overlap in polarisation responses, particularly in real environment with high diversity of particles.

4 Discussion

The results presented in this paper (Figs. 2, 5 and S3, S4 in the Supplement) illustrate the ability of the CASPOL instrument to provide reliable Particle Size Distribution (PSD) in expansion chamber campaigns, and to classify atmospheric particles of different phases, viscosities, shapes, and sizes. The polarisation ratio was combined with the PBP clustering technique to highlight the time resolved aspherical fraction evolution. Although there are known limitations and uncertainties in these measurements, e.g., particle sedimentation (Chapter 6 in Kulkarni, 2011), electronic “ringing”, and leakage currents (Kramer, 2002), they did not affect the filtered results (Fig. 3b) shown here.

the classification map presented here to discriminate between different kinds of atmospheric particles (e.g., ice crystals, ammonium sulphate, volcanic ash, SOA) will allow better insight for atmospheric transport and chemical processes.

5 Conclusions

5 The CLOUD 8–9 campaigns at the CERN facility, introduced a new capability of this facility for cloud particle measurements (Cloudy). In this paper the first CASPOL Cloudy measurements of mixed phase and ice clouds are presented. We discuss the advantages of particle by particle analysis of the polarisation. Single-particle polarisation was used here to discriminate water, ice, SOA, and other atmospheric particles. The capability to detect viscous oxidized alpha-pinene with the CASPOL is reported for the first time.

We present observation of reversed transition from liquid to viscous based on CASPOL, SMPS measurements, and SOA modelling. In our experiments, the SOA viscous to liquid transition is shown to be a reversible process. This result contributes to our understanding of viscous SOA appearance in the atmosphere, ageing and potentially to the solar radiation budget calculations.

15 Classification using the clustering technique produced a classification map that can contribute to future chamber and, possibly, atmospheric measurements of small particles with CASPOL in a heterogeneous environment. Small ice particles formed during different stages of the cloud still pose a great challenge for the optical instruments. Future efforts will focus on classification of additional cloud particles using CASPOL.

20 **The Supplement related to this article is available online at doi:10.5194/acpd-15-31433-2015-supplement.**

Discrimination of water, ice and aerosols by light polarisation

L. Nichman et al.

Title Page

Abstract

Introduction

Conclusions

References

Tables

Figures



Back

Close

Full Screen / Esc

Printer-friendly Version

Interactive Discussion



Acknowledgements. We would like to thank CERN for supporting CLOUD with important technical and financial resources, and for providing a particle beam from the CERN Proton Synchrotron. We express great appreciation for the CLOUD collaboration and the volunteers for the night shifts. We would also like to thank Darrel Baumgardner for CASPOL data filtering advice and review of the manuscript. T. B. Kristensen gratefully acknowledges funding from the German Federal Ministry of Education and Research (BMBF) through the CLOUD12 project. This research has received funding from the EC Seventh Framework Programme (Marie Curie Initial Training Network “CLOUD-TRAIN” no. 316 662) and Swiss National Science Foundation (SNSF) grant no. 200 021_140 663.

References

- Baran, A.: Light scattering by irregular particles in the Earth's atmosphere, in: Light Scattering Reviews 8, edited by: Kokhanovsky, A. A., Springer Praxis Books, Berlin, Heidelberg, Germany, 3–68, 2013.
- Baumgardner, D., Jonsson, H., Dawson, W., O'Connor, D., and Newton, R.: The cloud, aerosol and precipitation spectrometer: a new instrument for cloud investigations, *Atmos. Res.*, 59, 251–264, doi:10.1016/S0169-8095(01)00119-3, 2001.
- Baumgardner, D., Brenguier, J. L., Bucholtz, A., Coe, H., DeMott, P., Garrett, T. J., Gayet, J. F., Hermann, M., Heymsfield, A., Korolev, A., Krämer, M., Petzold, A., Strapp, W., Pilewskie, P., Taylor, J., Twohy, C., Wendisch, M., Bachalo, W., and Chuang, P.: Airborne instruments to measure atmospheric aerosol particles, clouds and radiation: a cook's tour of mature and emerging technology, *Atmos. Res.*, 102, 10–29, doi:10.1016/j.atmosres.2011.06.021, 2011.
- Benz, S., Megahed, K., Möhler, O., Saathoff, H., Wagner, R., and Schurath, U.: T-dependent rate measurements of homogeneous ice nucleation in cloud droplets using a large atmospheric simulation chamber, *J. Photoch. Photobio. A*, 176, 208–217, doi:10.1016/j.jphotochem.2005.08.026, 2005.
- Berkemeier, T., Shiraiwa, M., Pöschl, U., and Koop, T.: Competition between water uptake and ice nucleation by glassy organic aerosol particles, *Atmos. Chem. Phys.*, 14, 12513–12531, doi:10.5194/acp-14-12513-2014, 2014.

Discrimination of water, ice and aerosols by light polarisation

L. Nichman et al.

Title Page

Abstract

Introduction

Conclusions

References

Tables

Figures



Back

Close

Full Screen / Esc

Printer-friendly Version

Interactive Discussion



Discrimination of water, ice and aerosols by light polarisation

L. Nichman et al.

Title Page

Abstract

Introduction

Conclusions

References

Tables

Figures



Back

Close

Full Screen / Esc

Printer-friendly Version

Interactive Discussion

and Ariya, P. A., Topics in Current Chemistry, Springer, Berlin, Heidelberg, Germany, 97–143, 2014.

Dias, A., Ehrhart, S., Vogel, A., Williamson, C., Simões, J., Kirkby, J., Mathot, S., and Onnela, A.: Analysis of temperature homogeneity of the CLOUD chamber at CERN, in preparation, 2015.

Duplissy, J., Enghoff, M. B., Aplin, K. L., Arnold, F., Aufmhoff, H., Avngaard, M., Baltensperger, U., Bondo, T., Bingham, R., Carslaw, K., Curtius, J., David, A., Fastrup, B., Gagné, S., Hahn, F., Harrison, R. G., Kellelt, B., Kirkby, J., Kulmala, M., Laakso, L., Laaksonen, A., Lillestol, E., Lockwood, M., Mäkelä, J., Makhmutov, V., Marsh, N. D., Nieminen, T., Onnela, A., Pedersen, E., Pedersen, J. O. P., Polny, J., Reichl, U., Seinfeld, J. H., Sipilä, M., Stozhkov, Y., Stratmann, F., Svensmark, H., Svensmark, J., Veenhof, R., Verheggen, B., Viisanen, Y., Wagner, P. E., Wehrle, G., Weingartner, E., Wex, H., Wilhelmsson, M., and Winkler, P. M.: Results from the CERN pilot CLOUD experiment, *Atmos. Chem. Phys.*, 10, 1635–1647, doi:10.5194/acp-10-1635-2010, 2010.

Duplissy, J., DeCarlo, P. F., Dommen, J., Alfarra, M. R., Metzger, A., Barmpadimos, I., Prevot, A. S. H., Weingartner, E., Tritscher, T., Gysel, M., Aiken, A. C., Jimenez, J. L., Canagaratna, M. R., Worsnop, D. R., Collins, D. R., Tomlinson, J., and Baltensperger, U.: Relating hygroscopicity and composition of organic aerosol particulate matter, *Atmos. Chem. Phys.*, 11, 1155–1165, doi:10.5194/acp-11-1155-2011, 2011.

Fahey, D. W., Gao, R.-S., Möhler, O., Saathoff, H., Schiller, C., Ebert, V., Krämer, M., Peter, T., Amarouche, N., Avallone, L. M., Bauer, R., Bozóki, Z., Christensen, L. E., Davis, S. M., Durr, G., Dyroff, C., Herman, R. L., Hunsmann, S., Khaykin, S. M., Mackrodt, P., Meyer, J., Smith, J. B., Spelten, N., Troy, R. F., Vömel, H., Wagner, S., and Wienhold, F. G.: The AquaVIT-1 intercomparison of atmospheric water vapor measurement techniques, *Atmos. Meas. Tech.*, 7, 3177–3213, doi:10.5194/amt-7-3177-2014, 2014.

Froyd, K. D., Murphy, D. M., Lawson, P., Baumgardner, D., and Herman, R. L.: Aerosols that form subvisible cirrus at the tropical tropopause, *Atmos. Chem. Phys.*, 10, 209–218, doi:10.5194/acp-10-209-2010, 2010.

Glen, A. and Brooks, S. D.: A new method for measuring optical scattering properties of atmospherically relevant dusts using the Cloud and Aerosol Spectrometer with Polarization (CASPOL), *Atmos. Chem. Phys.*, 13, 1345–1356, doi:10.5194/acp-13-1345-2013, 2013.

Discrimination of water, ice and aerosols by light polarisation

L. Nichman et al.

Title Page

Abstract

Introduction

Conclusions

References

Tables

Figures



Back

Close

Full Screen / Esc

Printer-friendly Version

Interactive Discussion



mala, M., Stratmann, F., Worsnop, D. R., Möhler, O., Leisner, T., and Schnaiter, M.: Observation of viscosity transition in α -pinene secondary organic aerosol, *Atmos. Chem. Phys. Discuss.*, 15, 28575–28617, doi:10.5194/acpd-15-28575-2015, 2015.

Jimenez, J. L., Canagaratna, M. R., Donahue, N. M., Prevot, A. S. H., Zhang, Q., Kroll, J. H., DeCarlo, P. F., Allan, J. D., Coe, H., Ng, N. L., Aiken, A. C., Docherty, K. S., Ulbrich, I. M., Grieshop, A. P., Robinson, A. L., Duplissy, J., Smith, J. D., Wilson, K. R., Lanz, V. A., Hueglin, C., Sun, Y. L., Tian, J., Laaksonen, A., Raatikainen, T., Rautiainen, J., Vaattovaara, P., Ehn, M., Kulmala, M., Tomlinson, J. M., Collins, D. R., Cubison, M. J., E., Dunlea, J., Huffman, J. A., Onasch, T. B., Alfarra, M. R., Williams, P. I., Bower, K., Kondo, Y., Schneider, J., Drewnick, F., Borrmann, S., Weimer, S., Demerjian, K., Salcedo, D., Cottrell, L., Griffin, R., Takami, A., Miyoshi, T., Hatakeyama, S., Shimono, A., Sun, J. Y., Zhang, Y. M., Dzepina, K., Kimmel, J. R., Sueper, D., Jayne, J. T., Herndon, S. C., Trimborn, A. M., Williams, L. R., Wood, E. C., Middlebrook, A. M., Kolb, C. E., Baltensperger, U., and Worsnop, D. R.: Evolution of organic aerosols in the atmosphere, *Science*, 326, 1525–1529, doi:10.1126/science.1180353, 2009.

Johnson, B., Turnbull, K., Brown, P., Burgess, R., Dorsey, J., Baran, A. J., Webster, H., Haywood, J., Cotton, R., Ulanowski, Z., Hesse, E., Woolley, A., and Rosenberg, P.: In situ observations of volcanic ash clouds from the FAAM aircraft during the eruption of Eyjafjallajökull in 2010, *J. Geophys. Res.-Atmos.*, 117, D00U24, doi:10.1029/2011JD016760, 2012.

Kaye, P. H., Hirst, E., Greenaway, R. S., Ulanowski, Z., Hesse, E., DeMott, P. J., Saunders, C., and Connolly, P.: Classifying atmospheric ice crystals by spatial light scattering, *Opt. Lett.*, 33, 1545–1547, doi:10.1364/OL.33.001545, 2008.

Kirkby, J., Curtius, J., Almeida, J., Dunne, E., Duplissy, J., Ehrhart, S., Franchin, A., Gagne, S., Ickes, L., Kurten, A., Kupc, A., Metzger, A., Riccobono, F., Rondo, L., Schobesberger, S., Tsagkogeorgas, G., Wimmer, D., Amorim, A., Bianchi, F., Breitenlechner, M., David, A., Dommen, J., Downard, A., Ehn, M., Flagan, R. C., Haider, S., Hansel, A., Hauser, D., Jud, W., Junninen, H., Kreissl, F., Kvashin, A., Laaksonen, A., Lehtipalo, K., Lima, J., Lovejoy, E. R., Makhmutov, V., Mathot, S., Mikkilä, J., Minginette, P., Mogo, S., Nieminen, T., Onnela, A., Pereira, P., Petaja, T., Schnitzhofer, R., Seinfeld, J. H., Sipila, M., Stozhkov, Y., Stratmann, F., Tome, A., Vanhanen, J., Viisanen, Y., Vrtala, A., Wagner, P. E., Walther, H., Weingartner, E., Wex, H., Winkler, P. M., Carslaw, K. S., Worsnop, D. R., Baltensperger, U., and Kulmala, M.: Role of sulphuric acid, ammonia and galactic cosmic rays in atmospheric aerosol nucleation, *Nature*, 476, 429–433, 2011.

**Discrimination of
water, ice and
aerosols by light
polarisation**

L. Nichman et al.

Title Page

Abstract

Introduction

Conclusions

References

Tables

Figures



Back

Close

Full Screen / Esc

Printer-friendly Version

Interactive Discussion



Koop, T., Bookhold, J., Shiraiwa, M., and Pöschl, U.: Glass transition and phase state of organic compounds: dependency on molecular properties and implications for secondary organic aerosols in the atmosphere, *Phys. Chem. Chem. Phys.*, 13, 19238–19255, doi:10.1039/C1CP22617G, 2011.

5 Kramer, J.: An integrated optical transient sensor, *Circuits and Systems II: Analog and Digital Signal Processing*, *IEEE Transactions on Circuits and Systems – II*, 49, 612–628, doi:10.1109/TCSII.2002.807270, 2002.

Krämer, M.: HALO ice crystal spectrometer intercomparison at the AIDA-chamber: first results from the Novel Ice Experiment NIXE-CAPS, *Geophys. Res. Abstr.*, Vol. 11, EGU General Assembly, Vienna, Austria, 2009.

10 Kulkarni, G., Pekour, M., Afchine, A., Murphy, D. M., and Cziczo, D. J.: Comparison of experimental and numerical studies of the performance characteristics of a pumped counterflow virtual impactor, *Aerosol Sci. Tech.*, 45, 382–392, doi:10.1080/02786826.2010.539291, 2011.

15 Lance, S.: Coincidence errors in a Cloud Droplet Probe (CDP) and a Cloud and Aerosol Spectrometer (CAS), and the improved performance of a modified CDP, *J. Atmos. Ocean. Tech.*, 29, 1532–1541, doi:10.1175/JTECH-D-11-00208.1, 2012.

Lawson, R. P. B., Baker, B. A., and Pilson, B. A.: In-situ measurements of microphysical properties of mid-latitude and anvil cirrus, in: *Proceedings, 30th International Symposium on Remote Sensing Environment*, Honolulu, Hawaii, 10–14 November, 707–710, 2003.

20 Macke, A., Mueller, J., and Raschke, E.: Single scattering properties of atmospheric ice crystals, *J. Atmos. Sci.*, 53, 2813–2825, doi:10.1175/1520-0469(1996)053<2813:SSPOAI>2.0.CO;2, 1996.

Meyer, J.: Ice crystal measurements with SIMONE and CAS DPOL, Ph.D. thesis, Julich Forschungszentrum, Wuppertal, Germany, 140 pp., 2011.

25 Mikhailov, E., Vlasenko, S., Martin, S. T., Koop, T., and Pöschl, U.: Amorphous and crystalline aerosol particles interacting with water vapor: conceptual framework and experimental evidence for restructuring, phase transitions and kinetic limitations, *Atmos. Chem. Phys.*, 9, 9491–9522, doi:10.5194/acp-9-9491-2009, 2009.

30 Möhler, O., Field, P. R., Connolly, P., Benz, S., Saathoff, H., Schnaiter, M., Wagner, R., Cotton, R., Krämer, M., Mangold, A., and Heymsfield, A. J.: Efficiency of the deposition mode ice nucleation on mineral dust particles, *Atmos. Chem. Phys.*, 6, 3007–3021, doi:10.5194/acp-6-3007-2006, 2006.

**Discrimination of
water, ice and
aerosols by light
polarisation**

L. Nichman et al.

Title Page

Abstract

Introduction

Conclusions

References

Tables

Figures



Back

Close

Full Screen / Esc

Printer-friendly Version

Interactive Discussion



Noma, Y. and Asakawa, Y.: Biotransformation of monoterpenoids by microorganisms, insects, and mammals, in: Handbook of Essential Oils: Science, Technology, and Applications, CRC Press, Boca Raton, FL, USA, 585–736, 2010.

Omar, A. H., Won, J.-G., Winker, D. M., Yoon, S.-C., Dubovik, O., and McCormick, M. P.: Development of global aerosol models using cluster analysis of Aerosol Robotic Network (AERONET) measurements, *J. Geophys. Res.-Atmos.*, 110, D10S14, doi:10.1029/2004JD004874, 2005.

Pandis, S. N., Harley, R. A., Cass, G. R., and Seinfeld, J. H.: Secondary organic aerosol formation and transport, *Atmos. Environ. A-Gen.*, 26, 2269–2282, doi:10.1016/0960-1686(92)90358-R, 1992.

Petzold, A., Esselborn, M., Weinzierl, B., Ehret, G., Ansmann, A., Müller, D., Donovan, D., van Zadelhoff, G.-J., Berthier, S., Wiegner, M., Gasteiger, J., Buras, R., Mayer, B., Lajas, D., and Wehr, T.: ICAROHS inter-comparison of aerosol retrievals and observational requirements for multi-wavelength HSRL systems, in: Proceedings of the ESA Living Planet Symposium, Bergen, Norway, 28 June–2 July 2010, edited by: Lacoste-Francis, H., Vol. SP-686 (European Space Agency, 2010), p. 102, 2010.

Renbaum-Wolff, L., Grayson, J. W., Bateman, A. P., Kuwata, M., Sellier, M., Murray, B. J., Shilling, J. E., Martin, S. T., and Bertram, A. K.: Viscosity of alpha-pinene secondary organic material and implications for particle growth and reactivity, *P. Natl. Acad. Sci. USA*, 110, 8014–8019, doi:10.1073/pnas.1219548110, 2013.

Robinson, E. S., Saleh, R., and Donahue, N. M.: Organic aerosol mixing observed by single-particle mass spectrometry, *J. Phys. Chem. A*, 117, 13935–13945, doi:10.1021/jp405789t, 2013.

Rosenberg, P. D., Dean, A. R., Williams, P. I., Dorsey, J. R., Minikin, A., Pickering, M. A., and Petzold, A.: Particle sizing calibration with refractive index correction for light scattering optical particle counters and impacts upon PCASP and CDP data collected during the Fennec campaign, *Atmos. Meas. Tech.*, 5, 1147–1163, doi:10.5194/amt-5-1147-2012, 2012.

Schnaiter, M.: The Ice Cloud Characterisation Campaign HALO-02, *Geophys. Res. Abstr.*, Vol. 11, EGU General Assembly, Vienna, Austria, 2009.

Schnaiter, M., Büttner, S., Möhler, O., Skrotzki, J., Vragel, M., and Wagner, R.: Influence of particle size and shape on the backscattering linear depolarisation ratio of small ice crystals – cloud chamber measurements in the context of contrail and cirrus microphysics, *Atmos. Chem. Phys.*, 12, 10465–10484, doi:10.5194/acp-12-10465-2012, 2012.

Tajiri, T., Yamashita, K., Murakami, M., Saito, A., Kusunoki, K., Orikasa, N., and Lilie, L.: A novel adiabatic-expansion-type cloud simulation chamber, *J. Meteorol. Soc. Jpn.*, 91, 687–704, doi:10.2151/jmsj.2013-509, 2013.

5 Wiberg, K. B., Wang, Y.-G., Murphy, M. J., and Vaccaro, P. H.: Temperature dependence of optical rotation: α -pinene, β -pinene pinane, camphene, camphor and fenchone, *J. Phys. Chem. A*, 108, 5559–5563, doi:10.1021/jp040085g, 2004.

Discrimination of water, ice and aerosols by light polarisation

L. Nichman et al.

Title Page

Abstract

Introduction

Conclusions

References

Tables

Figures



Back

Close

Full Screen / Esc

Printer-friendly Version

Interactive Discussion



Discrimination of water, ice and aerosols by light polarisation

L. Nichman et al.

Title Page

Abstract

Introduction

Conclusions

References

Tables

Figures



Back

Close

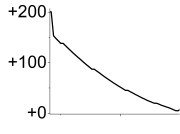
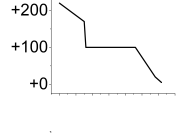
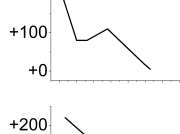
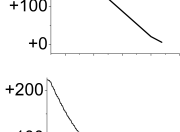
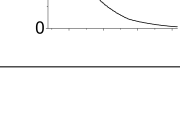
Full Screen / Esc

Printer-friendly Version

Interactive Discussion



Table 1. Experimental parameters of the expansion runs presented in this paper. Excess pressure profile x axis is of the order of several minutes.

Run#	Seed type	Seed concentration [cm^{-3}]	Excess Pressure profile [mb]	T_{initial} [$^{\circ}\text{C}$]	$\text{RH}_{\text{ice}}^{\text{max}}$ [%]
1248.13	Ammonium Sulphate	3000		+10	107
1291.16	Sulphuric Acid	75		-30	168, 135
1298.20	Sulphuric Acid	700		-50	148
1311.03	Sulphuric Acid	3260		-10	123
1471.34	Oxalic Acid	100		-20	165

Discrimination of water, ice and aerosols by light polarisation

L. Nichman et al.

Title Page

Abstract

Introduction

Conclusions

References

Tables

Figures



Back

Close

Full Screen / Esc

Printer-friendly Version

Interactive Discussion

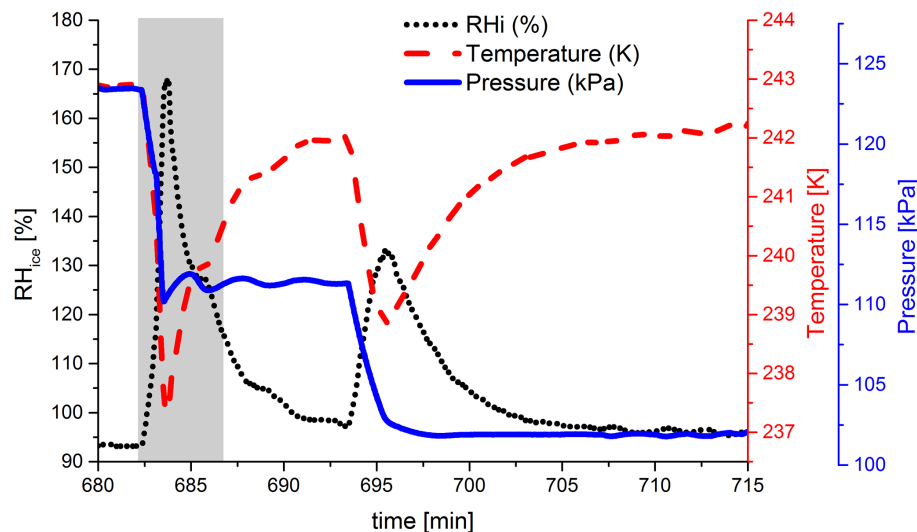


Figure 1. Example of programmable multistep expansion to form a mixed phase cloud (Run #1291.16). Relative humidity with respect to ice (RH_{ice}) calculated from MBW and Thermocouples. Second step grows the present ice particles in the cloud period (~ 25 min). Shaded time period is analysed in Fig. 3.

Discrimination of water, ice and aerosols by light polarisation

L. Nichman et al.

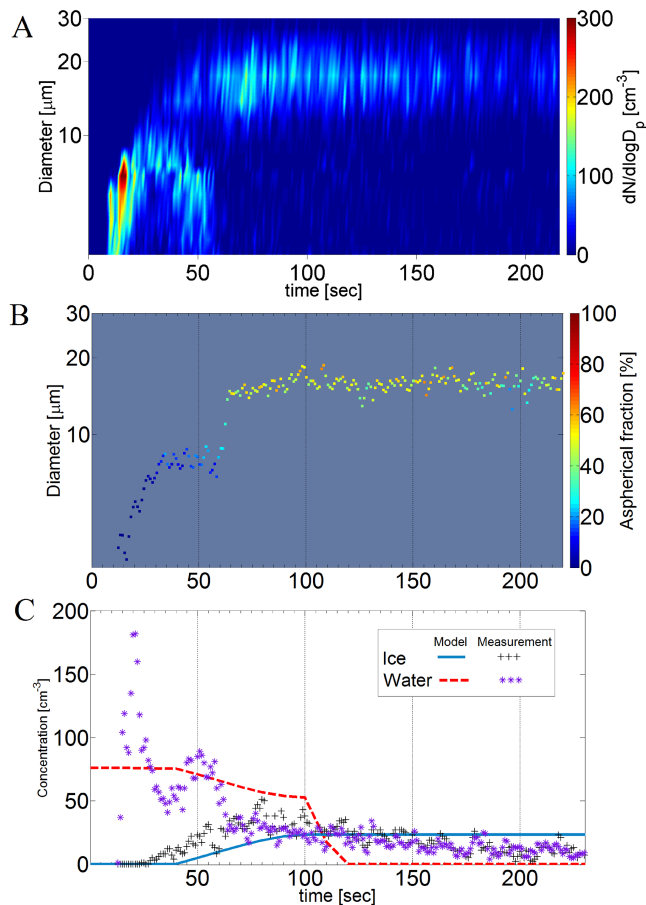


Figure 2. Mixed phase cloud, phase transition period (Run #1291.16). **(a)** CASPOL particle size distribution, **(b)** CASPOL PBP aspherical fraction, **(c)** CASPOL measured water and ice concentrations derived from asphericity compared to ACPIM.

Discrimination of water, ice and aerosols by light polarisation

L. Nichman et al.

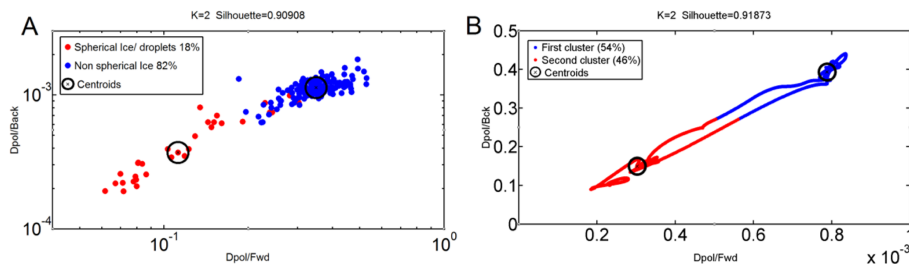


Figure 3. Cluster analysis (Run #1291.16). K in the title indicates the number of clusters found with best silhouette value. Each cluster appears with a percentage of particles in it. The centres of clusters are marked by centroids \otimes . **(a)** 1 s averaged data, whole size range and all concentration, **(b)** particle by particle data clustering for selected size range and concentration thresholds.

Title Page

Abstract

Introduction

Conclusions

References

Tables

Figures

◀

▶

◀

▶

Back

Close

Full Screen / Esc

Printer-friendly Version

Interactive Discussion



Discrimination of water, ice and aerosols by light polarisation

L. Nichman et al.

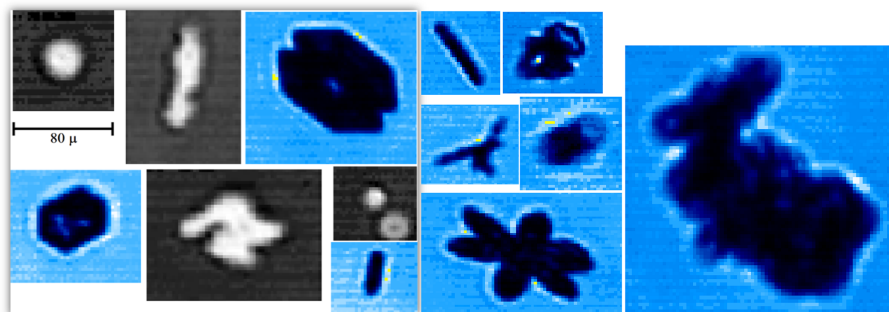


Figure 4. Images of ice particles in CLOUD captured by 3VCPI with $2\ \mu\text{m}$ resolution. Most of the particles are smaller than $100\ \mu\text{m}$ (scale on the left).

Title Page

Abstract

Introduction

Conclusions

References

Tables

Figures



Back

Close

Full Screen / Esc

Printer-friendly Version

Interactive Discussion



Discrimination of water, ice and aerosols by light polarisation

L. Nichman et al.

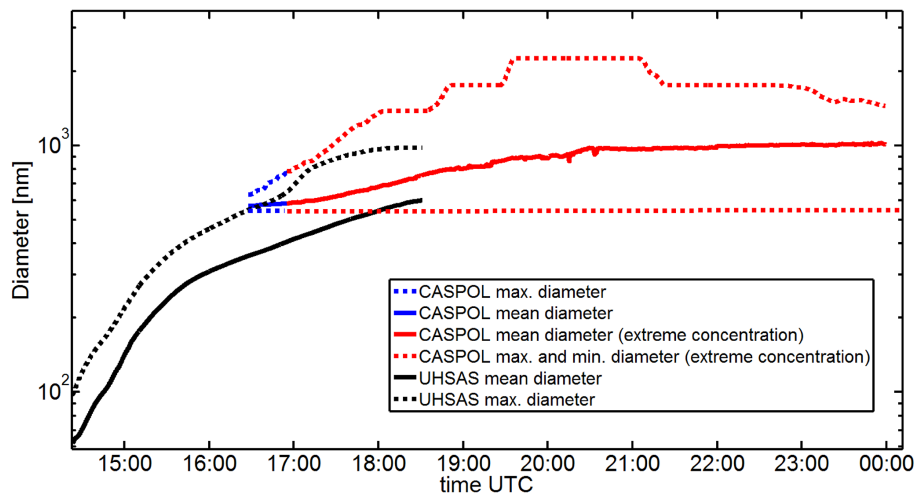


Figure 5. SOA growth over a 10 h period, 1 Hz sampling rate (Run #1516). CASPOL and UHSAS overlapped size measurements. Black lines – particles measured with UHSAS, instrument's cut-off is at 1000 nm. Blue lines – particles measured with CASPOL. Red lines indicate that CASPOL has passed the saturation threshold and the measurements may be subject to coincidence errors.

[Title Page](#)[Abstract](#)[Introduction](#)[Conclusions](#)[References](#)[Tables](#)[Figures](#)[◀](#)[▶](#)[◀](#)[▶](#)[Back](#)[Close](#)[Full Screen / Esc](#)[Printer-friendly Version](#)[Interactive Discussion](#)

Discrimination of water, ice and aerosols by light polarisation

L. Nichman et al.

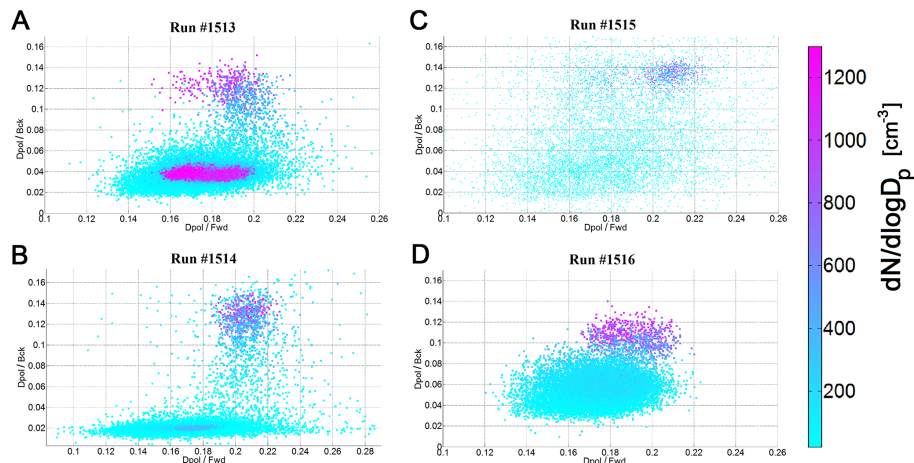


Figure 6. Polarisation scatter-plots of SOA growth and liquefaction measured by CASPOL in four experiments. Ratio of perpendicularly polarised backscatter intensity to total backscatter intensity ($D_{\text{pol}}/B_{\text{ck}}$) vs. ratio of perpendicularly polarised backscatter to forward scatter intensity ($D_{\text{pol}}/F_{\text{wd}}$), 1 s averaged run periods where the concentration was below 1300 cm^{-3} , colour is concentration $dN/d\log D_p$ (cm^{-3}), (a) Run #1513, (b) Run #1514, (c) Run #1515, (d) Run #1516.

[Title Page](#)
[Abstract](#)
[Introduction](#)
[Conclusions](#)
[References](#)
[Tables](#)
[Figures](#)
[◀](#)
[▶](#)
[◀](#)
[▶](#)
[Back](#)
[Close](#)
[Full Screen / Esc](#)
[Printer-friendly Version](#)
[Interactive Discussion](#)

Discrimination of water, ice and aerosols by light polarisation

L. Nichman et al.

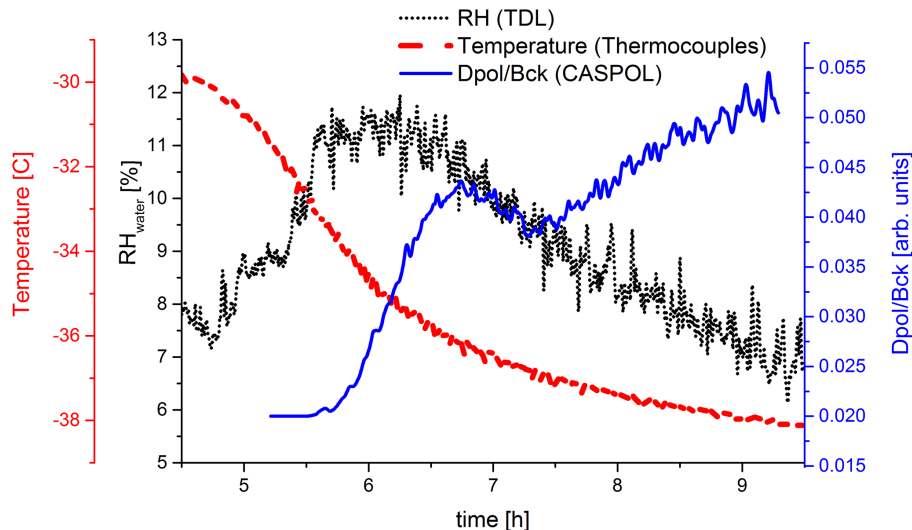


Figure 7. CASPOL polarisation ratio (blue line) increases as RH (black dotted line) decreases during the cooling period after a SOA experiment (Run #1515.16).

[Title Page](#)[Abstract](#)[Introduction](#)[Conclusions](#)[References](#)[Tables](#)[Figures](#)[◀](#)[▶](#)[◀](#)[▶](#)[Back](#)[Close](#)[Full Screen / Esc](#)[Printer-friendly Version](#)[Interactive Discussion](#)

Discrimination of water, ice and aerosols by light polarisation

L. Nichman et al.

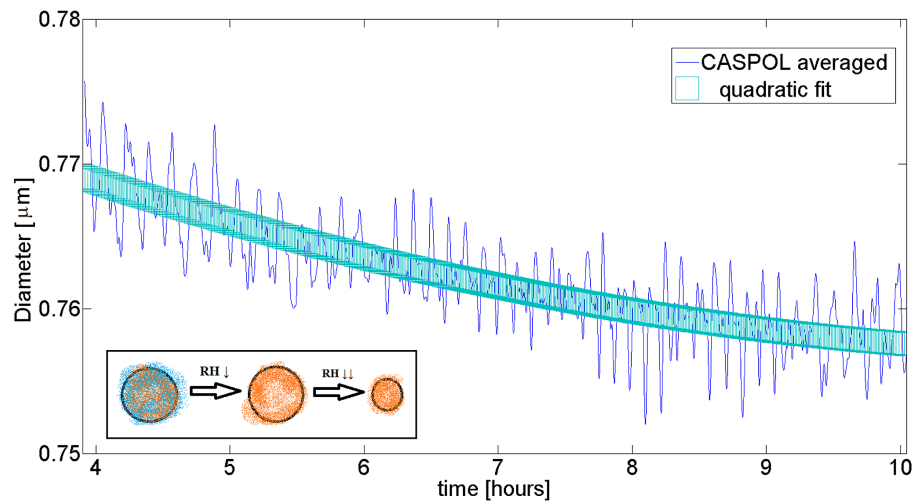


Figure 8. Large dry particles decrease in size. Smaller frame: illustration of the hypothesised transition sequence from CASPOL and SMPS measurements (liquid to viscous and dried further).

[Title Page](#)[Abstract](#)[Introduction](#)[Conclusions](#)[References](#)[Tables](#)[Figures](#)[◀](#)[▶](#)[◀](#)[▶](#)[Back](#)[Close](#)[Full Screen / Esc](#)[Printer-friendly Version](#)[Interactive Discussion](#)

Discrimination of water, ice and aerosols by light polarisation

L. Nichman et al.

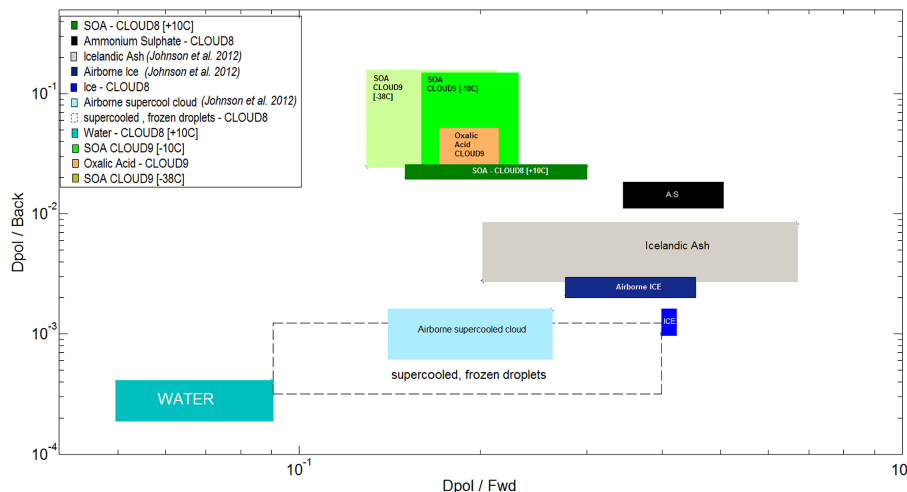


Figure 9. Atmospheric particle classification map for CLOUD data. The dimensions of the coloured rectangular boxes represent the space of measurements error and data points' distribution. Additional CASPOL data points from aircraft measurements are presented for comparison (Johnson et al., 2012).

Title Page

Abstract

Introduction

Conclusions

References

Tables

Figures

◀

▶

◀

▶

Back

Close

Full Screen / Esc

Printer-friendly Version

Interactive Discussion

